Self-consistent atomic orbital computation and visualization

Qian Zhang

The study of atomic orbitals plays an important role in understanding the intrinsic properties of atoms. In this report, we first discuss how to compute atomic orbitals for a one-electron system numerically. Then we generalize the problem to many-electron systems to obtain solutions in the self-consistent field approximation. In the end, we implement Monte-Carlo sampling to visualize the computed orbitals in three-dimensional space.

0.1 Introduction

Atoms, which are the fundamental building blocks in nature, directly govern all the physical and chemical properties of matter. To understand materials, we must understand individual atoms. One of the most important and interesting problem is to study how the electrons are distributed around the nucleus, i.e. the structure of atomic orbitals.
To compute atomic orbitals, the problem is to solve the Schrödinger equation

$$H\psi = E\psi \tag{0.1}$$

where H, the Hamiltonian of the system, is given by

$$H = \sum_{i=1}^{N}\left[-\frac{\hbar^2}{2m_e}\nabla_i^2 - \frac{1}{4\pi\epsilon_0}\frac{Ze^2}{r_i}\right] + \sum_{i<j}\frac{1}{4\pi\epsilon_0}\frac{e^2}{|\vec{r}_i - \vec{r}_j|} \tag{0.2}$$

The term in the bracket represents the kinetic plus potential energy of the ith electron, experiencing the attraction from the heavy nucleus of charge Ze. The last term, which complicates the behavior of the system, describes the electron-electron repulsions among all N electrons.
Eqn. (0.1) is basically an eigenvalue problem. The resulting eigen-energies E, are the possible total energies of the system. The corresponding eigen-functions ψ, are the many-electron wave functions that describe the electron distributions in the space.

0.2 One-electron system

0.2.1 Radial equation and angular equation

To start with, we consider the simplest case: a one-electron or hydrogen-like system. For $N = 1$, Eqn. (0.1) reads

$$\left[-\frac{\hbar^2}{2m_e}\nabla^2 - \frac{1}{4\pi\epsilon_0}\frac{Ze^2}{r}\right]\psi = E\psi \tag{0.3}$$

In spherical coordinates, by separation of variables $\psi(r,\theta,\phi) = R(r)Y(\theta,\phi)$, Eqn. (0.3) splits into two equations, namely,

$$\text{Radial equation:}\quad \frac{1}{R}\frac{d}{dr}\left(r^2\frac{dR}{dr}\right) - \frac{2m_e r^2}{\hbar^2}\left[-\frac{1}{4\pi\epsilon_0}\frac{Ze^2}{r} - E\right] = l(l+1) \tag{0.4}$$

$$\text{Angular equation:}\quad \frac{1}{Y}\left[\frac{1}{\sin\theta}\frac{\partial}{\partial\theta}\left(\sin\theta\frac{\partial Y}{\partial\theta}\right) + \frac{1}{\sin^2\theta}\frac{\partial^2 Y}{\partial\phi^2}\right] = l(l+1) \tag{0.5}$$

where l is the angular momentum quantum number (non-negative integer).
The angular equation is simple. Eqn. (0.5) does not depend on the potential and is the same for all atoms. The exact solutions for $Y(\theta,\phi)$ are the well known spherical harmonics [1].
The more difficult task is to solve the radial equation. Eqn. (0.4) simplifies if we change variables $u(r) \equiv rR(r)$. The radial equation becomes

$$\boxed{-\frac{\hbar^2}{2m_e}\frac{d^2u}{dr^2} + \left[-\frac{1}{4\pi\epsilon_0}\frac{Ze^2}{r} + \frac{\hbar^2}{2m_e}\frac{l(l+1)}{r^2}\right]u = Eu} \tag{0.6}$$

with boundary conditions: $u(r) \propto r^{l+1}$ as $r \to 0$ and $u(r) \propto e^{-r}$ as $r \to \infty$.
Eqn. (0.6) looks like a one-dimensional Schrödinger equation, where we have a "centrifugal" term $(\hbar^2/2m_e)[l(l+1)/r^2]$ in addition to the potential from the nucleus attraction. The problem is to solve this equation for $u(r)$ and the corresponding E. For this simplest one-electron system, the solution is known analytically [1]. Nevertheless, we will solve this equation numerically so that we can further deal with the more general case, the many-electron system.

0.2.2 Choice of units

Before we start to solve Eqn. (0.6), it is useful to pay attention to the choice of units. Obviously, we can use the SI units, but the scale would be a problem. For example, in SI units, the reduced Planck constant reads $\hbar = 1.054572 \times 10^{-34}\,\mathrm{J \cdot s}$, which is a crazy number from a computational point of view. Hence, we employ atomic units, namely,

$$\begin{aligned} \text{Length:} \quad & 1\ \mathrm{a_0} \approx 5.2918 \times 10^{-11}\ \mathrm{m} \\ \text{Mass:} \quad & 1\ \mathrm{m_e} \approx 9.1095 \times 10^{-31}\ \mathrm{kg} \\ \text{Time:} \quad & 1\ \mathrm{t_0} \approx 2.4189 \times 10^{-17}\ \mathrm{s} \\ \text{Charge:} \quad & 1\ \mathrm{e} \approx 1.6022 \times 10^{-19}\ \mathrm{C} \end{aligned}$$

which are deliberately chosen such that

$$\begin{aligned} \hbar &= 1\ \mathrm{a_0^2 m_e t_0^{-1}} \\ m_e &= 1\ \mathrm{m_e} \\ e &= 1\ \mathrm{e} \\ 4\pi\epsilon_0 &= 1\ \mathrm{a_0^{-3} m_e t_0^2 e^2} \end{aligned}$$

By adopting atomic units, the radial equation in (0.6) simplifies to

$$-\frac{1}{2}\frac{d^2u}{dr^2} + \left[-\frac{Z}{r} + \frac{1}{2}\frac{l(l+1)}{r^2}\right] u = Eu \tag{0.7}$$

This is how we implement the equation in the program. Distances are given in units of the Bohr radius ($\mathrm{a_0}$) and energies in Hartree ($\mathrm{a_0^2 m_e t_0^{-2}}$).

0.2.3 Numerical method

We are now in a position to solve the differential equation in (0.7) numerically. It is often convenient to solve problems on uniform grids. However, the curvature of the wave function (second derivative) $u'' = 2\left[-\frac{Z}{r} + \frac{1}{2}\frac{l(l+1)}{r^2} - E\right] u$ indicates that the function $u(r)$ oscillates faster if r goes smaller. This suggests us to take more points for small r but fewer for large r. For instance, Fig. 0.1 depicts the exact solution $u_{40}(r)$ for a hydrogen atom ($Z = 1$) on three different 25-point grids. Comparing Fig. 0.1a and 0.1b, we observe that a higher resolution close to the nucleus is desired.
Our choice is to use a logarithmic grid [2], $0 < r_0 < r_1 < \cdots < r_{n-1} < \infty$, where

$$r_i = \frac{1}{Z} e^{x_i} \tag{0.8}$$

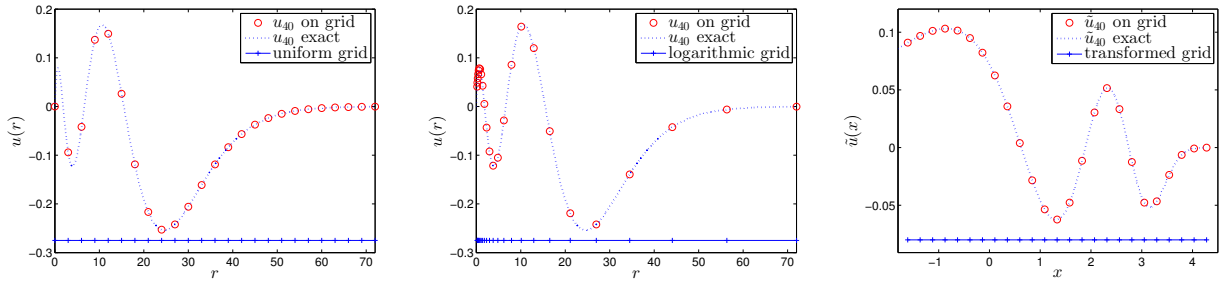

(a) u_{40} on a uniform grid (b) u_{40} on a logarithmic gird (c) $\tilde{u}_{40}$ on a transformed grid

Figure 0.1: Exact solution u_{40} for a hydrogen atom on 25-point grids. (a) u_{40} on a uniform grid; (b) u_{40} on a logarithmic grid; (c) $\tilde{u}_{40}$ on a transformed gird.

and x is a uniformly distributed grid

$$x_i = x_0 + i\Delta x \tag{0.9}$$

The problem on the logarithmic grid r (Fig. 0.1b) can be easily transformed to a problem on the uniform grid x (Fig. 0.1c) by a change of variable $u(r) = u(e^x/Z)$. Introducing a rescaled quantity $\tilde{u} \equiv u/\sqrt{r}$, one can show that Eqn. (0.7) transforms to

$$-\frac{1}{2}\frac{d^2\tilde{u}}{dx^2} + \left[-rZ + \frac{1}{2}\left(l+\frac{1}{2}\right)^2\right]\tilde{u} = r^2 E\tilde{u} \tag{0.10}$$

The second derivative in the equation above can be written in the finite-difference form

$$\frac{d^2\tilde{u}}{dx^2} \approx \frac{\tilde{u}_{i+1} - 2\tilde{u}_i + \tilde{u}_{i-1}}{\Delta x^2} \tag{0.11}$$

From Eqn. (0.10) and (0.11), we obtain

$$\tilde{u}_{i+1} = \left\{2 + 2\Delta x^2\left[-r_i Z + \frac{1}{2}\left(l+\frac{1}{2}\right)^2 - r_i^2 E\right]\right\}\tilde{u}_i - \tilde{u}_{i-1} \tag{0.12}$$

This is a simple recursion. We first initialize $\tilde{u}_0$ and $\tilde{u}_1$ according to their asymptote $\tilde{u} \propto r^{l+1}/\sqrt{r}$ as $r \to 0$. Then we obtain $\tilde{u}_2$, $\tilde{u}_3$, $\cdots$, $\tilde{u}_{n-1}$ from the recursion above. Note that the energy E is an unknown. To determine the energy, we implement the shooting method [3] to find E such that $\tilde{u}_{n-1} \to 0$. For instance, we compute the first few radial wave functions of a hydrogen atom. In this problem we take $r_0 = 0.001$, $r_{n-1} = 150.0$ and $\Delta x = 0.001$. The numerical results $R(r) = u(r)/r = \tilde{u}(r)/\sqrt{r}$ are shown in Fig. 0.2.

0.3 Many-electron system

0.3.1 Self-consistent field approximation

In the previous section we successfully implemented a numerical method to solve the one-electron system. A more general question is to solve the cases where multiple electrons orbit around the nucleus, i.e. the many-electron system.

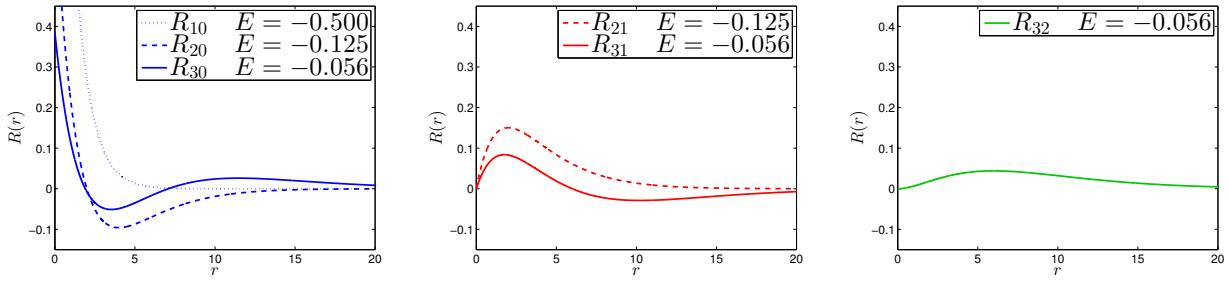

(a) R_{10}, R_{20} and R_{30} (b) R_{21} and R_{31} (c) R_{32}

Figure 0.2: Numerical results of the first few radial wave functions of a hydrogen atom. (a) first three radial wave functions with $l = 0$; (b) first two radial wave functions with $l = 1$; (c) the first radial wave function with $l = 2$

Recall our many-electron Hamiltonian in Eqn. (0.2). The Schrödinger equation gives

$$\left\{\sum_{i=1}^{N}\left[-\frac{\hbar^2}{2m_e}\nabla_i^2 - \frac{1}{4\pi\epsilon_0}\frac{Ze^2}{r_i}\right] + \sum_{i<j}\frac{1}{4\pi\epsilon_0}\frac{e^2}{|\vec{r}_i - \vec{r}_j|}\right\}\psi = E\psi \tag{0.13}$$

Unfortunately, this equation cannot be solved exactly. The electron-electron interactions make the system extremely difficult to analyze. Actually, even if we can solve Eqn. (0.13), the resulting many-electron wave function $\psi(\vec{r}_1, \vec{r}_2, \ldots, \vec{r}_N)$ will be an extremely huge object that is not possible to store on an ordinary hard disc. Consequently, the self-consistent field (SCF) method was developed to treat this problem approximately.
The idea of the SCF method is to take a mean-field potential to approximate the electron-electron repulsions. The exact Hamiltonian

$$H = \sum_{i=1}^{N}\left[-\frac{\hbar^2}{2m_e}\nabla_i^2 - \frac{1}{4\pi\epsilon_0}\frac{Ze^2}{r_i}\right] + \underbrace{\sum_{i<j}\frac{1}{4\pi\epsilon_0}\frac{e^2}{|\vec{r}_i - \vec{r}_j|}}_{\text{trouble maker}} \tag{0.14}$$

is approximated by

$$H_0 = \sum_{i=1}^{N}\left[-\frac{\hbar^2}{2m_e}\nabla_i^2 - \frac{1}{4\pi\epsilon_0}\frac{Ze^2}{r_i}\right] + V_H(r) \tag{0.15}$$

where $V_H(r)$ is called the Hartree potential.
Under this approximation, the many-electron problem $\psi(\vec{r}_1, \vec{r}_2, \ldots, \vec{r}_N)$ dramatically breaks down to one-electron problems $\psi_1(\vec{r}), \psi_2(\vec{r}), \ldots, \psi_N(\vec{r})$ which we already know how to solve. Eqn. (0.13) now becomes

$$\left\{\left[-\frac{\hbar^2}{2m_e}\nabla^2 - \frac{1}{4\pi\epsilon_0}\frac{Ze^2}{r}\right] + V_H(r)\right\}\psi_i = E_i\psi_i \quad \text{for } i = 1, 2, \cdots, N \tag{0.16}$$

for which the radial equation we are going to solve is

$$\boxed{-\frac{\hbar^2}{2m_e}\frac{d^2u_i}{dr^2} + \left[-\frac{1}{4\pi\epsilon_0}\frac{Ze^2}{r} + \frac{\hbar^2}{2m_e}\frac{l(l+1)}{r^2} + V_H(r)\right]u_i = E_iu_i} \quad \text{for } i = 1, 2, \cdots, N \tag{0.17}$$

It is identical to Eqn. (0.6) except that we have an additional Hartree potential $V_H(r)$.
The Hartree potential is the mean-field Coulomb potential created by all electrons. Each electron contributes a part of the Hartree potential

$$V_H(r) = \sum_{i=1}^{N} V_i(r) \tag{0.18}$$

Assuming spherical symmetric distributions of electrons, the potential contribution from each electron is simply given by

$$V_i(r) = \frac{1}{4\pi\epsilon_0} e \int_r^{\infty} \frac{Q_i(r')}{r'^2} dr' \tag{0.19}$$

where $Q_i(r) = e\int_0^r u_i^2(r')dr'$ is the electron charge enclosed in the sphere of radius r.
Now we encounter a dilemma:

- To compute the $\{u_i(r)\}$, we need $V_H(r)$
- To compute $V_H(r)$, we need the $\{u_i(r)\}$

This "chicken-or-egg" problem can be solved by an iterative scheme as illustrated in Fig. 0.3. We start from an initial guess of the Hartree potential, say, $V_H^0(r) = 0$. From this initial guess, we obtain a solution $\{u_i^0(r)\}$. Next, we use this solution to update $V_H^1(r)$ and obtain a new solution $\{u_i^1(r)\}$. This loop continues until the Hartree potential $V_H^k(r)$ and solution $\{u_i^k(r)\}$ converge. That is why this scheme is called self-consistent field method: $\{u_i(r)\}$ produces $V_H(r)$ and $V_H(r)$ results in $\{u_i(r)\}$, which is self-consistent.

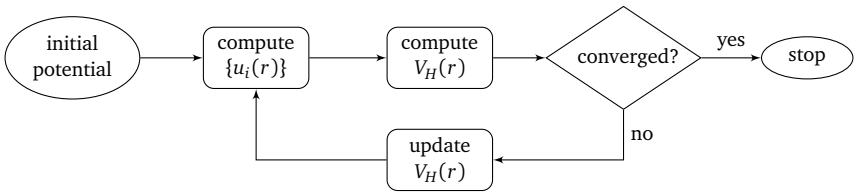

Figure 0.3: Flow chart of self-consistent field iteration. The loop starts from an initial potential and continues updating the Hartree potential until the solution converges.

0.3.2 Exchange-correlation correction

The mean-field approximation works well for most of the atoms. However, in some cases, the solution may not converge. A more accurate (and robust) computation requires an exchange-correlation term in addition to the Hartree term. The approximated Hamiltonian is given in the form

$$H_0 = \sum_{i=1}^{N} \left[-\frac{\hbar^2}{2m_e}\nabla_i^2 - \frac{1}{4\pi\epsilon_0}\frac{Ze^2}{r_i} \right] + V_H(r) + V_{xc}(r) \tag{0.20}$$

$V_{xc}(r)$ is a subtle correction. The idea behind is the density functional theory (DFT), which exactly maps the many-electron problem onto equivalent one-electron problems. In practical calculations, the local density approximation (LDA) is usually used to simplify the computation for this exchange-correlation term. There are many different functional approximations to compute $V_{xc}(r)$, but we will not explicitly list them here. A detailed discussion can be found in the reference [4].

0.3.3 Self-consistent field computation results

As an example, we demonstrate the SCF computation results for a carbon atom. A carbon atom has 6 electrons, with corresponding electronic configuration: $1s^2\ 2s^2\ 2p^2$. The computation starts with zero electron-electron interaction. Fig. 0.4a shows the first iteration solution assuming non-interacting electrons. Fig. 0.4b plots the second iteration solution with updated Hartree potential and exchange-correlation correction. We observe that the wave functions are shifted away from the nucleus (mainly the "outer" electrons) as a result of the electron-electron repulsion, and the corresponding eigen-energies increase. The iteration continues until we see there is no observable difference between iteration 15 and 20. Then we conclude that the self-consistency is achieved and we obtained the radial wave function for a carbon atom.

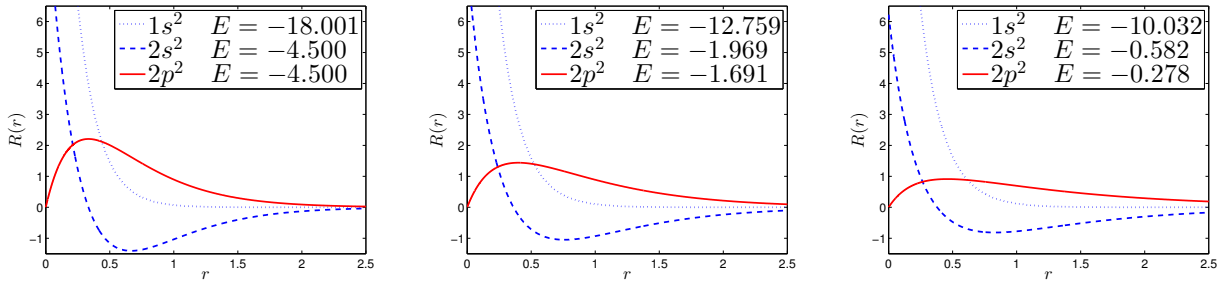

(a) Iteration = 1 (b) Iteration = 2 (c) Iteration = 5

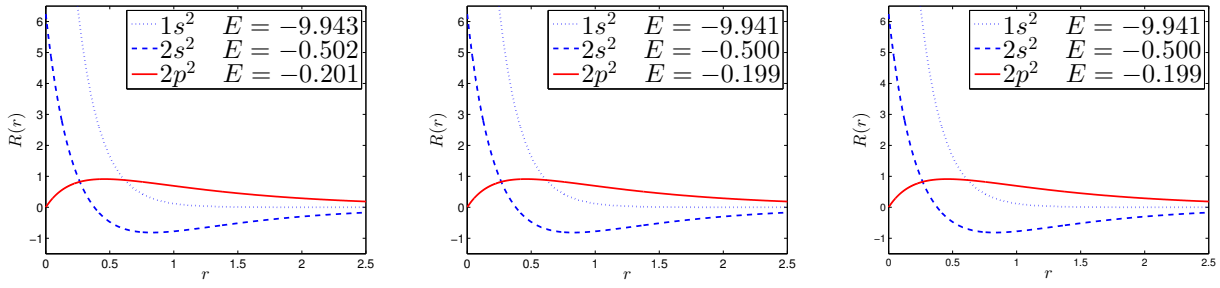

(d) Iteration = 10 (e) Iteration = 15 (f) Iteration = 20

Figure 0.4: Self-consistent field computation results for a carbon atom. From (a) to (f) the wave functions and eigen-energies approach the converged solution. The solution converges after about 15 iterations.

0.4 Atomic orbital visualization

0.4.1 Monte-Carlo sampling

As promised in the beginning, we are now going to visualize the atomic orbitals from the previous computations. An atomic orbital $\psi(r, \theta, \phi)$ consists of two parts, $R(r)$ and $Y(\theta, \phi)$. The radial part $R(r)$, which we have spent a lot of effort on, is obtained from the self-consistent field approximation. The angular part $Y(\theta, \phi)$, which we don't need to worry about, is well known as the spherical harmonics and its computation routine can be easily found in the book *Numerical Recipes* [5].

It is not trivial to visualize a three-dimensional function $\psi(r,\theta,\phi)$ as it would require four axes r, θ, ϕ and ψ to plot the object. Therefore, we perform Monte-Carlo sampling to visualize $\psi(r,\theta,\phi)$ in a probabilistic approach. Taking the radial function $R_{42}(r)$ of a silver atom as an example, the idea is the following:

1. Generate a random point under the sampling curve (Fig. 0.5);
2. If this point falls into the shaded region $|R_{42}(r)|$, we accept the coordinate r of this point. Otherwise, this point is rejected;
3. Repeat the sampling many times. The density of the points represents the value of the function $|R_{42}(r)|$.

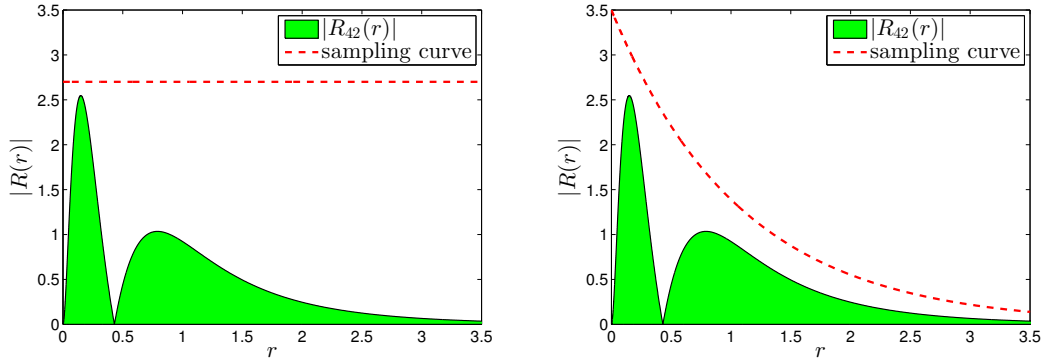

(a) Uniform sampling (b) Weighted sampling

Figure 0.5: Monte-Carlo sampling for the radial part $R_{42}(r)$. If the point falls into the shaded region, we accept the r of this point. (a) inefficient uniform sampling; (b) efficient weighted sampling.

The choice of the sampling curve strongly affects the efficiency of the scheme [6]. The simplest way is to perform a uniform sampling, in which only uniform random number generation is required. However, as shown in Fig. 0.5a, this method results in a huge waste of rejected points due to the exponential decay of the wave function. A more suitable sampling curve is an exponential function $Ae^{-\beta r}$, which properly envelopes the wave function (Fig. 0.5b).
To determine the parameters A and β for the sampling curve, we need the information from the radial wave function. Say, a function $R_{nl}(r)$ with eigen-energy E, we determine the decaying factor as $\beta = \sqrt{-2m_e E}/\hbar$, which is suggested from the analytical solution of the one-electron system [1]. The amplitude A is determined such that the sampling curve can enclose the entire wave function with minimum A.
A similar idea applies to the sampling for the angular part $Y(\theta,\phi)$, but with a much simpler sampling curve (well, surface if you like), a uniform sphere. Fig. 0.6 illustrates the sampling for a spherical harmonics $Y_{20}(\theta,\phi)$ on the x-z cut plane. If the point falls into the shaded region, we accept the θ and ϕ of this point.

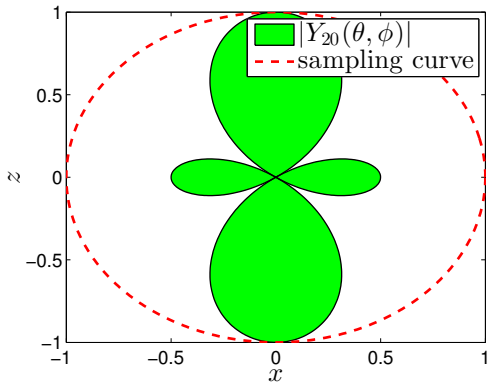

Figure 0.6: Monte-Carlo sampling for the angular part $Y_{20}(\theta,\phi)$ (x-z cut plane). If the point falls into the shaded region, we accept the θ and ϕ of this point.

0.5 Visualization results

The combination of radial and angular sampling gives us the density plot of the atomic orbital.

$$\text{Radial part } R(r) \times \text{Angular part } Y(\theta,\phi) = \text{Atomic orbtial } \psi(r,\theta,\phi)$$

Fig. 0.7 demonstrates the visualization results for the $4s$ orbital of a potassium (K) atom, the $4p_z$ orbital of a bromine (Br) atom, the $4d_{3z^2-1}$ orbital of a silver (Ag) atom and the $5f_{y(3x^2-y^2)}$ orbital of a uranium (U) atom. The orbitals are colored in red if the wave function is positive and in blue if is negative. In the atomic orbital plots (right), higher density of points represents a larger absolute value of the wave function $\psi(r,\theta,\phi)$, which implies there will be a higher probability to find an electron in that region.

0.6 Conclusion

Starting from the simplest case, we solved the one-electron system numerically on a logarithmic grid. Then we generalized the problem into many-electron systems to compute the solution from the self-consistent field approximation. Finally, we successfully performed a weighted Monte-Carlo sampling to visualize atomic orbitals in three-dimensional space.

0.7 Acknowledgement

I am heartily thankful to my supervisor, Prof. Dr. Erik Koch, for his guidance, encouragement and support through my project period. I would like to thank German Research School for Simulation Sciences for sponsoring my project and Jülich Supercomputing Center for providing me this great research opportunity. Special thanks to Dr. Ivo Kabadshow for organizing this excellent guest student programme.

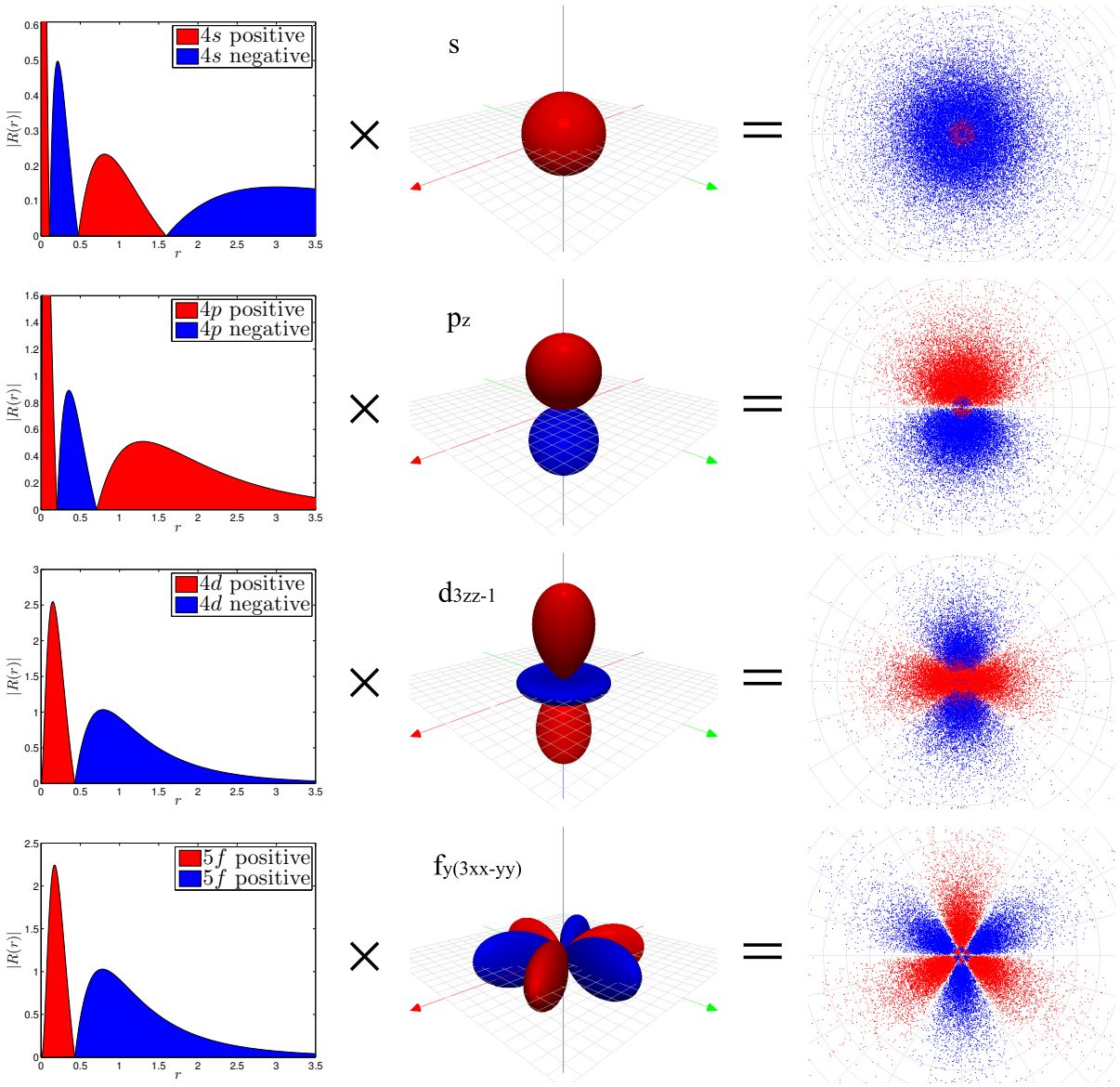

Figure 0.7: Orbital visualizations for a potassium atom (1st row), a bromine atom (2nd row), a silver atom (3rd row) and a uranium atom (4th row). (left) radial part; (middle) angular part; (right) atomic orbital. The orbitals are colored in red if the wave function is positive and in blue if is negative.

Bibliography

[1] D. J. Griffiths, *Introduction to quantum mechanics*, Pearson Prentice Hall (2005).

[2] R. M. Martin, *Electronic structure*, Cambridge University Press (2004).

[3] N. J. Giordano and H. Nakanishi, *Computational physics*, Pearson Prentice Hall (2006).

[4] J. M. MacLaren, D. P. Clougherty, M. E. McHenry and M. M. Donovan, *Parameterised local spin density exchange-correlation energies and potentials for electronic structure calculations*, Computer Physics Communications 66 (1991) 383–391.

[5] W. H. Press, S. A. Teukolsky, W. T. Vetterling and B. P. Flannery, *Numerical Recipes in C*, Cambridge University Press (1992).

[6] S. E. Koonin and D. C. Meredith, *Compututational physics*, Westview Press (1990).